Journal of Applied Electrochemistry **33**: 1011–1016, 2003.

Exploration of molten hydroxide electrochemistry for thermal battery applications

M.H. MILES
Chemistry Division, Research Department, Naval Air Warfare Center Weapons Division, China Lake, CA 93555, USA
(Present address: Department of Chemistry, University of La Verne, La Verne, CA 91750, USA; e-mail: mmiles@ulv.edu; Fax: +909 392 2754)

Received 12 November 2002; accepted in revised form 24 April 2003

Key words: cyclic voltammetry, electrostability window, reactions, reference electrodes, thermodynamics

Abstract

The electrochemistry of molten LiOH–NaOH, LiOH–KOH, and NaOH–KOH was investigated using platinum, palladium, nickel, silver, aluminum and other electrodes. The fast kinetics of the Ag^+/Ag electrode reaction suggests its use as a reference electrode in molten hydroxides. The key equilibrium reaction in each of these melts is $2\ OH^- = H_2O + O^{2-}$ where H_2O is the Lux-Flood acid (oxide ion acceptor) and O^{2-} is the Lux–Flood base. This reaction dictates the minimum H_2O content attainable in the melt. Extensive heating at 500 °C simply converts more of the alkali metal hydroxide into the corresponding oxide, that is, Li_2O, Na_2O or K_2O. Thermodynamic calculations suggest that Li_2O acts as a Lux–Flood acid in molten NaOH–KOH via the dissolution reaction $Li_2O_{(s)} + 2\ OH^- = 2\ LiO^- + H_2O$ whereas Na_2O acts as a Lux–Flood base, $Na_2O_{(s)} = 2\ Na^+ + O^{2-}$. The dominant limiting anodic reaction on platinum in all three melts is the oxidation of OH^- to yield oxygen, that is $2\ OH^- \rightarrow 1/2\ O_2 + H_2O + 2\ e^-$. The limiting cathodic reaction in these melts is the reduction of water in acidic melts ($[H_2O] \gg [O^{2-}]$) and the reduction of Na^+ or K^+ in basic melts. The direct reduction of OH^- to hydrogen and O^{2-} is thermodynamically impossible in molten hydroxides. The electrostability window for thermal battery applications in molten hydroxides at 250–300 °C is 1.5 V in acidic melts and 2.5 V in basic melts. The use of aluminum substrates could possibly extend this window to 3 V or higher. Preliminary tests of the Li–Fe (LAN) anode in molten LiOH–KOH and NaOH–KOH show that this anode is not stable in these melts at acidic conditions. The presence of superoxide ions in these acidic melts likely contributes to this instability of lithium anodes. Thermal battery development using molten hydroxides will likely require less active anode materials such as Li–Al alloys or the use of more basic melts. It is well established that sodium metal is both soluble and stable in basic NaOH–KOH melts and has been used as a reference electrode for this system.

1. Introduction

The first thermal batteries were developed by Germany during World War II for use in the V-1 and V-2 rockets and consisted of a calcium anode, a LiCl–KCl eutectic (m.p. 352 °C) electrolyte, and a $CaCrO_4$ cathode, that is, $Ca/LiCl–KCl/CaCrO_4$ [1, 2]. Thermal battery applications are still mainly limited to military missions, hence this technology has advanced slowly. The last major change in thermal batteries occurred in 1980 with the introduction of lithium or lithium-alloy anodes and the FeS_2 cathode, that is $Li/LiCl–KCl/FeS_2$. Currently, the all-lithium ternary salt, LiF–LiCl–LiBr (m.p. 430 °C), is generally used as the electrolyte in thermal batteries. Nevertheless, the cell voltage (2.0 V) and energy density (44 Wh kg^{-1}) remains low compared to other lithium batteries. Sophisticated missiles and weaponry today demand increasing electrical energy and power densities, thus present thermal battery technology is being pushed to its limits. New thermal battery materials yielding higher cell voltages and lower operating temperatures are needed. Another important parameter is a molten salt electrolyte with a high ionic conductivity that permits the high current densities needed for high power applications.

Table 1 presents a summary of key features of various molten salt systems. The main attractive features of NaOH–KOH are the relatively low melting point and the high ionic conductivity as well as the large liquid range (170–800 °C) offered by this melt. The ionic conductivity for NaOH–KOH at 227 °C (500 K) almost equals the value for LiCl–KCl at 450 °C. The LiOH–NaOH (m.p. 210 °C, 30 mol % LiOH) and LiOH–KOH (m.p. 226 °C, 31 mol % LiOH) eutectics also offer high ionic conductivities and large liquid temperature ranges. Electrochemical windows of 4 V or higher are found only for the nitrate melts. Likely thermal

Table 1. Properties of molten salt systems

System	Melting Point /°C	Conductivity* /S cm^{-1}	Electrochemical window† /V
$AlCl_3$–NaCl (63–37 mol %)	114	0.239 (175 °C)	2.2
$LiNO_3$–KNO_3 (43–57 mol %)	124	0.223 (177 °C)	4.5
NASCN–KSCN (26–74 mol %)	124	0.08 (162 °C)	1.8
$LiC_2H_3O_2$–$NaC_2H_3O_2$–$KC_2H_3O_2$ (20–30–50 mol %)	162	0.05 (222 °C)	2.0
NaOH–KOH (51–49 mol %)	170	1.40 (227 °C)	1.5–2.5
LiCl–KCl (59–41 mol %)	352	1.572 (450 °C)	3.6
Li_2CO_3–Na_2CO_3 (50–50 mol %)	496	1.73 (550 °C)	2.0
Li_2SO_4–K_2SO_4 (80–20 mol %)	535	1.282 (625 °C)	2.9
$NaPO_3$–KPO_3 (50–50 mol %)	628	–	0.95 (700 °C)

* Values from J.A. Plambeck, *in* A.J. Bard (Ed.), 'Encyclopedia of Electrochemistry of the Elements, Fused Salt Systems', Vol. 10, (Marcel Dekker, NY 1976).

† At the standard temperature given for conductivity.

battery applications using molten nitrates have been reported previously [3, 4].

2. Experimental details

The electrochemical studies employed a platinum cell that also served as the counter electrode. A silver wire sealed in shrinkable Teflon tubing was found to be suitable as a reference electrode for the purposes of this study. The electrochemistry of the molten hydroxides was investigated at temperatures between 250–300 °C controlled to within ±5 °C. A platinum working electrode was generally used, but studies were also made with nickel, silver, palladium, aluminium, magnesium, zinc and Li–Fe (LAN) electrodes. The electrode area was calculated from the length exposed to the hydroxide melt. The hydroxide eutectics were made by weighing out calculated amounts of Reagent grade LiOH (Matheson, Coleman and Bell, anhydrous), NaOH (Polarchem, 98.900%), and KOH (Fisher, 86.1%). The melts containing KOH obviously contained much more water, and this proved to be more difficult to remove than suggested by the literature [5]. Heating the fused LiOH–KOH or NaOH–KOH at 500 °C for 24 h did not adequately remove sufficient water to produce the basic melts. The LiOH–NaOH, LiOH–KOH, and NaOH–KOH melts were investigated after heating at 250–300 °C for several hours, after heating at 500 °C for 3 h and after heating at 500 °C for 24 h. Cyclic voltammetric and other electrochemical studies were conducted with the use of an EG&G (Perkin–Elmer) model 270 electrochemistry system with 250 Research Electrochemistry software. The cyclic voltammetric potential scans began and ended at 0.00 V vs Ag^+/Ag with the initial direction towards more negative potentials.

3. Results

No suitable reference electrode has been established for molten hydroxide systems [5–9]. However, the Ag^+/Ag reference electrode has been used in most of the molten salt systems shown in Table 1 [5], hence a Ag-wire reference electrode was selected for investigation in molten hydroxides. An important characteristic for a reference electrode is that it must have fast electrode kinetics reflected by a large exchange current density (i_o). For example, the H^+/H_2 electrode reaction in aqueous solutions at 25 °C has an exchange current density of $i_o = 10^{-3}$ A cm^{-2} on platinum electrodes. The cyclic voltammetric result for the Ag electrode ($A = 0.16$ cm^2) in molten NaOH–KOH at 280 °C is shown in Figure 1. The slow scan rate (1.00 mV s^{-1}) and the narrow potential range (±50 mV) allows determination of the exchange current density (i_o) from the equation

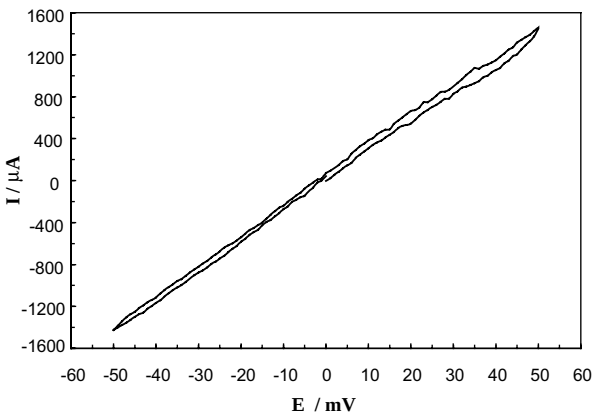

Fig. 1. Cyclic voltammetric study at 1.00 mV s^{-1} for the silver electrode ($A = 0.16$ cm^2) in molten NaOH–KOH at 280 °C.

$$i_o = RT/FR_{ct} = 8.5 \times 10^{-3}\ \mathrm{A\,cm^{-2}} \quad (1)$$

where the charge-transfer resistance (R_{ct}) is given by $R_{ct} = \Delta\eta/\Delta I$ and η is the overvoltage. This is a typical i_o value for a good reference electrode system and suggests that the Ag-wire reference should serve reasonably well for these studies. The exact nature of the Ag-wire reference electrode reaction in molten hydroxides is unknown. It may involve Ag^+/Ag, AgO_2/Ag or some other silver electrode reaction.

Figure 2 shows the cyclic voltammograms for a platinum electrode in this same NaOH–KOH melt at 280 °C. Despite heating this melt at 450–500 °C for more than 3 h, the cathodic limit near −1.3 V is still due to the reduction of H_2O, that is, $H_2O + e^- \rightarrow 1/2\ H_{2(g)} + OH^-$. Assuming that one-half of the water initially present was removed by the heating process, then the composition of this NaOH–KOH–H_2O melt would be 45–44–11 mol % ($pH_2O \cong -0.6$). The anodic limit near 0.2 V is due to the major oxidation in this melt and is likely the reaction $2\ OH^- \rightarrow 1/2\ O_{2(g)} + H_2O + 2\ e^-$ or possibly $4\ OH^- \rightarrow O_2^- + 2\ H_2O + 3e^-$ [8]. Gas evolution was visible at both the anodic and cathodic limits. The electrostability window for this acidic NaOH–KOH melt at 280 °C is thus 1.5 V. In the basic NaOH–KOH melt at 227 °C, the Na^+/Na reaction occurs at −2.3 V vs the Ag^+/Ag couple [5]. This is 1.0 V more negative than the limiting cathodic reaction shown in Figure 2.

An important feature of the cyclic voltammogram shown in Figure 2 is the large cathodic peak at −0.32 V. Furthermore, the current remains cathodic throughout the scan at potentials more negative than −0.1 V. This can be attributed to the reduction of superoxide ions, O_2^-, in the acidic NaOH–KOH melt, $O_2^- + 2\ H_2O + 3\ e^- \rightarrow 4\ OH^-$ [5]. The superoxide ion is formed by the reaction of atmospheric O_2 with OH^- in the melt, $3\ O_2 + 4\ OH^- \rightarrow 2\ H_2O + 4\ O_2^-$. This formation of O_2^- is reported to be essential in the preparation of superconducting $EuBa_2Cu_4O_8$ from molten hydroxides at 475 °C [10]. The reported standard potential of the O_2^-/OH^- couple in acidic NaOH–KOH at 227 °C is −0.03 V vs Ag^+/Ag [5]. Concentrations of O_2^- and H_2O less than 1 M would yield more negative potentials for this electrode reaction.

The effect of the potential scan rate on the O_2^-/OH^- reaction in this NaOH–KOH melt at 280 °C is summarized in Table 2. The excellent linear relationship between the peak current (I_p) and the square root of the potential scan rate ($v^{1/2}$) demonstrates that mass transport for the O_2^-/OH^- electrode reaction occurs under semi-infinite linear diffusion conditions ($I_p = 0.859 + 1.969\ v^{1/2}$, $R^2 = 0.998$).

Nickel crucibles containing molten NaOH form a protective black oxide film [5]. In this study, a nickel crucible used for heating LiOH–KOH at 500 °C became uniformly blackened, and the electrochemical studies of the melt did not show significant corrosion products. The cyclic voltammograms for a nickel electrode ($A = 0.34\ \mathrm{cm^2}$) in molten NaOH–KOH at 280 °C is shown in Figure 3. The nickel electrode is characterized by a sharp oxidation peak at −0.74 V that suggests the oxidation of a surface film. A black film was observed on the nickel electrode following these studies. A possible explanation is the oxidation of NiO to NiO_2, $NiO + 2OH^- \rightarrow NiO_2 + H_2O + 2e^-$. The standard potential of the $NiO_{2(s)}/NiO_{(s)}$ electrode reaction is given as −0.8 V vs Ag^+/Ag in acidic NaOH–KOH at 227 °C [5]. A puzzling feature, however, is that this oxidation peak nearly disappears when the cathodic potential scan is reversed at −1.1 V rather than at −1.3 V. Perhaps the regeneration of NiO requires the interaction of NiO_2 with hydrogen.

Table 2. Effect of the potential scan rate on E_p and I_p for the O_2^-/OH^- reaction in NaOH–KOH at 280 °C

Scan rate /mV s^{-1}	E_p /V	I_p /mA
20	−0.28	−10.1
50	−0.29	−14.5
100	−0.31	−21.6
200	−0.32	−28.0
500	−0.34	−46.2
1000	−0.37	−62.2

Platinum electrode area = 0.17 $\mathrm{cm^2}$.

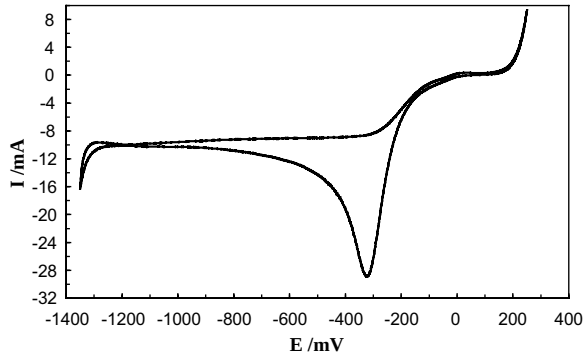

Fig. 2. Cyclic voltammetric study at 200 mV s^{-1} for the platinum electrode ($A = 0.17\ \mathrm{cm^2}$) in molten NaOH–KOH at 280 °C.

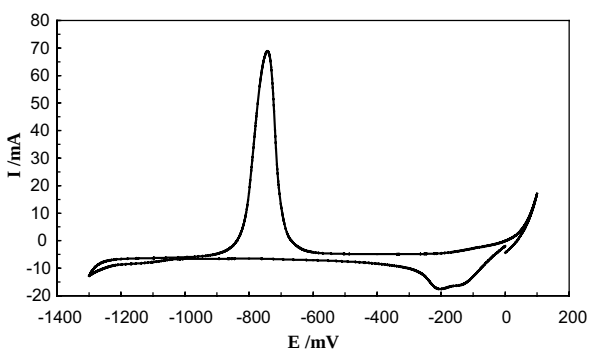

Fig. 3. Cyclic voltammetric study at 100 mV s^{-1} for the nickel electrode ($A = 0.34\ \mathrm{cm^2}$) in molten NaOH–KOH at 280 °C.

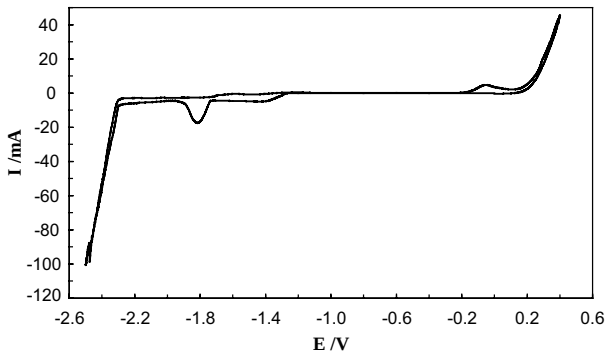

Fig. 4. Cyclic voltammetric study at 100 mV s^{-1} for the platinum electrode ($A = 0.15$ cm^2) in molten LiOH–NaOH at 270 °C.

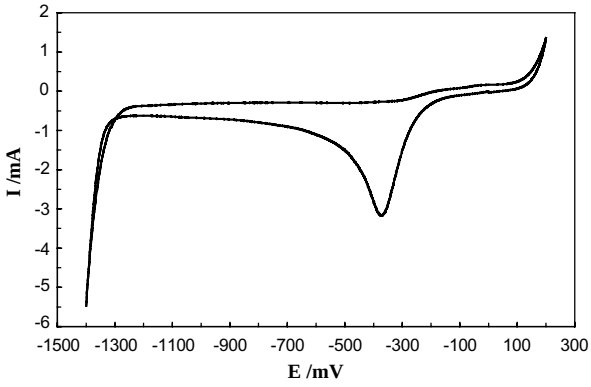

Fig. 5. Cyclic voltammetric study at 100 mV s^{-1} for the platinum electrode ($A = 0.15$ cm^2) in molten LiOH–KOH–LiCl (2 mol % LiCl) at 270 °C.

A typical cyclic voltammograms for the LiOH–NaOH melt at 270 °C using a platinum electrode is shown in Figure 4. There is obviously much less water in this melt, and the reduction of Na^+ begins near −2.3 V vs Ag^+/Ag. Some water, however, is present and contributes to the reduction beginning near −1.3 V. The irregular lines at high currents at the cathodic limit suggests that the deposited sodium is reacting with the water to produce hydrogen gas. Therefore, there is no observed oxidation of sodium during the reverse potential sweep. The major anodic wave begins near +0.2 V, thus an electrostability window of 2.5 V is available in this LiOH–NaOH melt.

Another striking feature of this LiOH–NaOH melt is that there is no cathodic peak for the O_2^-/OH^- electrode reaction. Furthermore, unlike the NaOH–KOH melt, the current remains very close to 0 mA over much of the potential scan. Obviously, there is very little reaction of atmospheric oxygen to form superoxide ions in this melt. The small size of the Li^+ ions apparently limits the spread of negative charge to other oxygen atoms to form O_2^{2-} or O_2^-. Similar effects are found in molten nitrates where significant O_2^{2-} or O_2^- forms in $NaNO_3$–KNO_3 but not in $LiNO_3$–KNO_3 [4, 5].

The third eutectic melt investigated was LiOH–KOH, and a representative cyclic voltammogram for platinum is shown in Figure 5. This melt also contained 2 mol % LiCl, but this third component had very little effect on the observed potentials or on the shape of the voltammogram. Because of the KOH component, this melt contained significant water despite the oven-drying at 500 °C for 24 h. Therefore, the electrochemical stability window is defined by the reduction of H_2O beginning near −1.35 V and the oxidation of OH^- beginning near 0.15 V to give a 1.5 V window. The reduction of superoxide ions is observed in this acidic melt, but the currents are considerably smaller than in the NaOH–KOH melt (Figure 2).

The palladium electrode was also investigated in the LiOH–KOH melt and yielded anodic and cathodic limits similar to platinum. However, the absorption of hydrogen into the palladium could be observed electrochemically even at high temperatures (280–300 °C). This suggests the possible use of the Pd–H system as a reference electrode in molten hydroxides.

Other electrode materials investigated in molten hydroxides include Al, Mg, Zn and Li–Fe (LAN) electrodes. The electrode area in each case was about 0.2 cm^2. Chronopotentiometric studies of Al in LiOH–NaOH at 270 °C yield the instrument limit of 10 V for $I = 20$ mA and the Na^+/Na potential of −2.3 V at $I = -20$ mA. This complete passivation of Al in molten hydroxides during the anodic scan may extend the electrostability window to 3 V or higher for battery applications in basic hydroxide melts. Although Mg yielded an open-circuit potential of −0.95 V in the LiOH–NaOH melt, it passivates readily with anodic currents. The Zn electrode gave an open-circuit potential of −0.7 V in the LiOH–NaOH melt, but it also passivated significantly with anodic currents. The Li–Fe (LAN) anode material proved too reactive in molten NaOH–KOH and in molten LiOH–KOH for any electrochemical studies. The high water content of these melts along with the presence of superoxide ions likely were the major cause of this reactivity. No Li–Fe anode studies were conducted in the LiOH–NaOH melt where the H_2O content was significantly smaller and the O_2^- species were nearly absent.

4. Discussion

Thermodynamic calculations can be used to gain significant insight into the chemistry and electrochemistry of molten hydroxides. For example, various standard electrode potentials and equilibrium constants are available for the NaOH–KOH melt at 500 K [5]. These can be combined to yield $\Delta G°$ and $E°$ values for other reactions. A reaction of special interest is

$$OH^- + e^- \rightarrow 1/2\ H_{2(g)} + O^{2-} \qquad (2)$$

that apparently does not occur in molten hydroxides. The $\Delta G°$ for this reaction can be obtained by adding the $\Delta G°$ values for the known reactions

$$2\ OH^- = H_2O + O^{2-} \quad (3)$$

$$H_2O + e^- \rightarrow 1/2\ H_{2(g)} + OH^- \quad (4)$$

The ΔG° value for Reaction 3 can be calculated from $K_{eq} = [H_2O][O^{2-}] = 3.16 \times 10^{-12}$ [5]. Using the convention of $E = 0.000$ V for the Na^+/Na couple [5] yields $\Delta G^\circ = 34.82$ kJ mol^{-1} for Reaction 2, thus $E^\circ = -0.361$ V vs Na^+/Na for this reaction or about $E^\circ = -2.66$ V vs Ag^+/Ag. Thermodynamically, sodium metal is stable in basic NaOH–KOH melts, and Reaction 2 is not possible. It follows that lithium metal is also likely stable in basic molten hydroxides and could be used as an anode material if the E° value for Li^+/Li is similar to that for Na^+/Na. However, the possible reaction of lithium metal with Na^+ or K^+ ions in basic molten hydroxides needs to be investigated. Less active anode materials such as Li–Al alloys may prove useful in the more acidic hydroxide melts.

The solubility product constant K_{sp}, can be thermodynamically calculated for the reaction

$$Na_2O_{(s)} = 2\ Na^+ + O^{2-} \quad (5)$$

by combining ΔG° values for the following three reactions at 500 K:

$$Na_2O_{(s)} \rightarrow 2\ Na_{(s)} + 1/2\ O_{2(g)} \quad (6)$$

$$2\ Na_{(s)} \rightarrow 2\ Na^+ + 2\ e^- \quad (7)$$

$$1/2\ O_{2(g)} + 2\ e^- \rightarrow O^{2-} \quad (8)$$

This yields $\Delta G^\circ = 17.23$ kJ mol^{-1} for Reaction 5, thus $K_{sp} = 1.58 \times 10^{-2}$. The calculated K_{sp} is smaller than the reported value of $K_{sp} = 34$ [5]. This is because the molar concentration of Na^+ (18.5 M) in the NaOH–KOH melt was used in the experimental calculation, and the activity of Na^+ is likely significantly less than its molar concentration.

The thermodynamic calculations for the reaction

$$PbO_{(s)} = Pb^{2+} + O^{2-} \quad (9)$$

yield $\Delta G^\circ = 114.22$ kJ mol^{-1} and $K_{sp} = 1.17 \times 10^{-12}$ in molten NaOH–KOH at 500 K. Experimental measurements for the reaction

$$Pb^{2+} + 2\ OH^- = PbO_{(s)} + H_2O \quad (10)$$

in NaOH–KOH at 500 K have been reported by Eluard and Trèmillon [11] that yield the acidity constant, $K_a = [H_2O]/[Pb^{2+}] = 2.6$. It can be readily shown that Reaction 3 minus Reaction 9 yields Reaction 10, thus this acidity constant can be expressed by $K_a = K_{eq}/K_{sp}$. The experimentally measured value of $K_a = 2.6$ yields $K_{sp} = 1.2 \times 10^{-12}$. This is indeed in close agreement with our thermodynamically calculated value of $K_{sp} = 1.17 \times 10^{-12}$.

The thermodynamic calculations for the solubility product for Li_2O, however, yields $\Delta G^\circ = 139.65$ kJ mol^{-1}, thus $K_{sp} = 2.57 \times 10^{-15}$. This differs significantly from the experimental value of $K_{sp} = 10^{-5}$ [5]. Reasonable agreement between the thermodynamic calculations and the experimental measurement are obtained if the solution reaction for Li_2O in molten NaOH–KOH at 500 K is given by

$$Li_2O_{(s)} + 2\ OH^- = 2\ LiO^- + H_2O \quad (11)$$

with $K_{sp} = [LiO^-]^2[H_2O] = 10^{-5}$. According to this equation, the equilibrium H_2O concentration in melts saturated with Li_2O would be 0.014 M. In contrast, the equilibrium H_2O concentration in NaOH–KOH melts saturated with Na_2O at 500 K would be 2.0×10^{-11} M ($pH_2O = 10.7$). Thus, Li_2O acts as a Lux–Flood acid (O^{2-} acceptor) in the NaOH–KOH melt while Na_2O acts as a Lux–Flood base. It can be shown from thermodynamics that the NaOH–KOH melt at 500 K saturated with both Li_2O and Na_2O will have an equilibrium H_2O content of 2×10^{-4} M. Thermodynamic calculations indicate that MgO also acts as Lux–Flood acid in molten NaOH–KOH. Lithium and magnesium compounds often show diagonal similarities.

These thermodynamic calculations suggest that in molten NaOH–KOH saturated with Na_2O, the H_2O content will be sufficiently small, and sodium or perhaps lithium could be used as anode materials. In fact, no passivating oxide film is needed to stabilize these active metal anodes in NaOH–KOH saturated with Na_2O. This thermodynamic conclusion has been verified experimentally by the use of sodium as a reference electrode in the basic NaOH–KOH melt [5]. Furthermore, the sodium metal is even somewhat soluble in this melt [5]. The presence of Li_2O, however, will lead to more acidic solutions. Based on the value $E^\circ = -0.361$ V vs Na^+/Na for Reaction 2, sodium metal will be thermodynamically stable in molten NaOH–KOH at 500 K for equilibrium H_2O concentrations less than 1.37×10^{-8} M. Procedures for removing undesirable peroxide and superoxide ions from molten alkali hydroxides have been presented by Claes et al. [12, 13].

Based on the fundamental equilibrium in molten hydroxides, $2\ OH^- = H_2O + O^{2-}$, continuous heating and removal of H_2O will simply convert more of the alkali metal hydroxide into its oxide. The heating of the NaOH–KOH melt in an atmosphere of dry nitrogen gas along with the addition of Na_2O has often been used to obtain the basic melt [8, 12–15].

5. Conclusions

Molten hydroxides offer the attractive properties of relatively low melting points, high ionic conductivities,

and wide liquid temperature ranges for possible thermal battery applications. The minimization of H_2O and O_2^- will likely be the key for the use of lithium or sodium anodes in these melts. Thermodynamic calculations lead to many useful conclusions regarding the chemistry and electrochemistry of molten hydroxides.

Acknowledgements

The author thanks J. Douglass Briscoe of SAFT America for providing the Li–Fe (LAN) anode material and Carl Hinners, Jennifer Irvin, and Geoff Lindsay of NAWCWD for this research opportunity.

References

1. V. Klasons, *in* D. Linden (Ed.), '*Handbook of Batteries*' (McGraw-Hill, New York, 2nd edn 1995), pp. 22.1–22.22.
2. M.H. Miles, Recent advances in lithium battery technology, *in* '*23rd Annual GaAs IC Symposium Technical Digest 2001*' IEEE, Piscataway, NJ (2001), pp. 219–222.
3. M.H. Miles, Lithium thermal batteries using molten nitrate electrolytes, *in* '*Proceedings of the 39th Power Sources Symposium*', Cherry Hill, NJ (2000), pp. 560–563.
4. M.H. Miles, Electrochemistry of molten nitrate electrolytes and applications for high voltage lithium cells, *in* '*Meeting Abstracts*', Vol. 2001–2, The Electrochemical Society, Pennington, NJ (2001), Abstract 125.
5. J.A. Plambeck, *in* A.J. Bard (Ed.), '*Encyclopedia of Electrochemistry of the Elements, Fused Salt Systems*', Vol. 10 (Marcel Dekker, NY 1976), pp. 283–318.
6. N. Saib, P. Claes and J. Glibert, *Electrochim. Acta* **43** (1998) 2089.
7. P. Claes, Y. Dewilde and J. Glibert, *J. Electroanal. Chem.* **250** (1988) 327.
8. P. Tilman, J.P. Wiaux, C. Dauby, J. Glibert and P. Claes, *J. Electroanal. Chem.* **167** (1984) 117.
9. J.P. Wiaux and P. Claes, *J. Electrochem. Soc.* **129** (1982) 123.
10. D. Sandford, L.N. Marquez and A.M. Stacy, *Appl. Phys. Lett.* **67** (1995) 422.
11. A. Eluard and B. Trèmillon, *J. Electroanal. Chem.* **30** (1971) 323.
12. P. Claes, F. Mernier, L. Wery and J. Glibert, *Electrochim. Acta* **44** (1999) 3999.
13. P. Claes, G. Peeters and J. Glibert, *J. Electrochem. Soc.* **136** (1989) 2599.
14. S. Zecchin, G. Schiavon and G.G. Bombi, *J. Electroanal. Chem.* **50** (1974) 261.
15. J. Goret and B. Trèmillon, *Bull. Soc. Chim. Fr* (1966) 67.